Hindawi Publishing Corporation
International Journal of Photoenergy
Volume 2009, Article ID 962783, 8 pages
doi:10.1155/2009/962783

Research Article

Nanosized TiO_2 Photocatalyst Powder via Sol-Gel Method: Effect of Hydrolysis Degree on Powder Properties

Nor Hafizah and Iis Sopyan

Department of Manufacturing and Materials Engineering, International Islamic University Malaysia (IIUM), P.O. Box 10, Kuala Lumpur 50728, Malaysia

Correspondence should be addressed to Iis Sopyan, sopyan@iiu.edu.my

Received 26 September 2008; Revised 20 January 2009; Accepted 8 April 2009

Recommended by Terry Egerton

Nanosized TiO_2 powder was synthesized via sol-gel method using titanium tetraisopoxide (TPT) as the precursor. Mol ratios of water to TPT were varied from 1 (Powder A), 2 (Powder B), 3 (Powder C), and 4 (Powder D) to evaluate effect of hydrolysis degree. TG/DTA curves showed that amorphous phase turned to anatase crystal structure at ca. 415, 337, 310, and 339°C for Powders A, B, C, and D, respectively. XRD analysis showed that all the synthesized TiO_2 powders were 100% in anatase form with Powders B and C showing considerably higher crystallinities. The powders obtained at lower water to TPT mol ratios were spherical in shape and they became bar-like shapes higher mol ratios. The lower hydrolysis degree led to higher surface area of the Powder A (24.8 m^2/g) compared to Powder B (14.6 m^2/g). From phenol photocatalytic measurement, Powder B was the most efficient attributed to its higher crystallinity.

1. Introduction

The rapid growth of industries especially in developed countries has lead to the expansion of environmental problems. An awful amount of hazardous waste are continuously released from factories into the uncontaminated river or ground water. An appropriate and a cheap technique to purify the contaminated waste water needs to be developed. Some conventional methods used to purify polluted waste water from the industries are by [1] (1) adsorption on activated carbon technique and (2) oxidative treatment by chlorine. In oxidative treatment, using chlorine is inefficient due to the formation of other toxic products due to the oxidation process such as desethylatrazine which is a degradation product from pesticide type of pollutant known as atrazine [1]. Other methods to remove organic pollutants in the water reported by Kansal et al. [2] were by employing chemical and physical processes such as precipitation, air stripping, flocculation, reverse osmosis, and ultrafiltration [2, 3]. Still, these techniques are nondestructive because they only transfer the nonbiodegradable matter into sludge that will only lead to formation of a new type of pollutant [2–4]. Other than these two conventional methods; a chemical oxidation method such as addition of potassium permanganate has also considerable potential to act as an oxidant to control biological growth in treatment plants, odor and taste as well as to remove colour. However, potassium permanganate is a poor disinfectant. It is also not advisable to leave a residual of potassium permanganate in purified water after the treatment as it can cause the colour of the water to turn to pink [5]. Potassium permanganate should also be handled with full body protection as it can cause serious injury to the eyes and can generate skin and inhalation irritant if direct contact is occurred. Thus, utilization of semiconductor photocatalyst is a promising approach and has been widely studied for treating the waste water containing harmful chemicals over the past three decades [6, 7].

Photocatalyst TiO_2 has been extensively used for environmental applications because of its high oxidative power, nontoxicity, photostability, and water insolubility properties under most conditions [6, 8–10]. Photocatalysis process uses ambient oxygen from air and irradiation, basically UV light, to generate oxidation and reduction which can degrade almost all harmful organic and inorganic compounds to

nontoxic substances. It is initiated when the amount of UV irradiation absorbs by TiO_2 transcends its band gap energy to induce the separation of electron from the valence band to the conduction band [11]. The electrons will react with the oxygen to produce superoxide anions and parallelly holes will react with water to produce the hydroxyl radicals to degrade and mineralize the organic compound [11]. TiO_2 with anatase crystal structure is more favorable than rutile as it is more active with band gap energy of 3.2 eV than rutile (3.0 eV) [12–14]. Higher surface area of TiO_2 anatase than rutile is another factor affecting its higher photocatalytic activity efficiency.

Several parameters need to be controlled in order to obtain a highly efficient degradation of organic molecules utilizing TiO_2 photocatalyst. Habibi et al. [15] have developed an efficient way to achieve the optimized photocatalyst process. The most optimal photocatalysis operational parameters such as oxygen, temperature, catalyst loading, UV-light irradiation time, solution pH, and inorganic ions were investigated for the complete decolorization of dyes. Vosooghian and Habibi [16] explained that the photooxidation process of organic sulfides using TiO_2 photocatalyst was better in the presence of pure oxygen rather than in atmospheric oxygen or in the absence of oxygen. The study proved that a specific and controlled oxidative chemistry in organic substrates adsorbed on TiO_2 surface was needed to achieve higher photodegradation rate of the pollutants. In another work, Habibi et al. [17] have also managed to develop TiO_2 thin film for dyes degradation. Investigation on the effect of annealing temperature on the dyes degradation rate found that the annealing temperature of thin film and the substrate nature on which TiO_2 films were deposited played important roles in enhancing the photocatalytic degradation rate of dyes. However, TiO_2 is not the only potential photocatalyst to carry out photodegradation process. Indium tin oxide thin film was one of the promising photocatalysts to degrade textile dyes to replace TiO_2 if the degradation process was done at the optimum condition [18].

In this work we have developed TiO_2 powder photocatalyst via sol-gel method using titanium tetraisopropoxide (TPT) as the precursor. TiO_2 photocatalyst powders with water-to-TPT mol ratios of 1, 2, 3, and 4 were synthesized. The effects of hydrolysis degree on the formation of powders particles were physicochemically investigated. It is expected that the amount of added water will affect the monomer hydrolysis rate resulting in formation of powder particles with different size and shape. The sol-gel derived TiO_2 powders were then tested to evaluate their photocatalytic efficiency in degradation of aqueous phenol solution as a representative model for polluted water.

2. Experimental

2.1. Synthesis of TiO_2 Powder. TiO_2 powders with water-to-TPT mol ratios of 1 (Powder A), 2 (Powder B), 3 (Powder C), and 4 (Powder D) were synthesized via sol-gel method. The synthesis was done by hydrolysis of titanium (IV) isopropoxide (TPT) (Sigma-Aldrich) as a precursor in methanol (R&M chemicals). Both chemicals were used as received. TPT and methanol were mixed and heated until boiling point of methanol was reached. Then, distilled water was added dropwise and it was left for several minutes to let the hydrolysis-polymerization process take place. The obtained white solution was filtered to get the precipitate of TiO_2 gel powder and dried at 200°C for 1 hour. The dried powder was calcined at 400°C for 1 hour to obtain crystalline sol-gel TiO_2 powder.

2.2. Characterization of TiO_2 Powder. The gel TiO_2 powders were characterized by thermogravimetric and differential thermal analysis (TG/DTA) (Pyris Diamond, Perkin Elmer) to determine the weight loss and phase changing of the powder. X-ray Diffractometer machine (XRD 6000, Shimadzu) was utilized for phase analysis. Fourier Transform Infrared (FTIR) (Spectrum 100, Perkin Elmer) was used to identify the existing bonds before and after calcination of TiO_2 powder. Powder particle size was measured by Zetasizer (Nano S, Malvern Instruments), and surface morphology was examined by a field emission scanning electron microscopy (FESEM) (JSM 6700F, JEOL). Surface area analysis of the powders was measured by a surface area analyzer (BET-Autosorb-1, Quantachrome Instrument). The change in phenol solution concentration was measured using UV-Vis spectrometer (Lambda 35, Perkin Elmer).

2.3. Phenol Degradation Experiment. The sol-gel TiO_2 powder in suspension form was used to degrade aqueous phenol solution. TiO_2 powder (5 g) was added into 250 mL phenol solution of 50 mg/L initial concentration. Phenol photodegradation process was carried out in a reactor consisting of black light bulbs with the wavelength of 369 nm as the UV source with intensity of 2.6 mW/cm^2. The suspension was magnetically stirred during photocatalytic test conducted for 5 hours. The sampling was done every one hour and the decrease in phenol solution concentration was measured by the UV-Vis spectrometer.

3. Results and Discussion

3.1. Photocatalyst Characterization. Figures 1, 2, 3, and 4 show the TG/DTA curves of TiO_2 Powders A, B, C, and D, respectively. From the TG curves, all powders show first weight loss at temperatures below 100°C, indicating that methanol and water started to evaporate from the powders [19–21]. At temperature of 100°C to 300°C, a weight loss of 14.4% for Powder A, 13.9% for Powder B, 22% for Powder C, and 19.7% for Powder D was recorded, which could be attributed to the removal of unhydrolyzed isopropoxide ligands bonded in the titanium. Meanwhile from the DTA curves, a sharp exothermic reaction peak appeared at ca. 414°C for Powder A, ca. 337°C for Powder B, ca. 310°C for Powder C, and ca. 399°C for Powder D indicating a phase change of the powder from amorphous to anatase phase. The powder crystallization temperature is summarized in Table 1. With its lower hydrolysis degree, Powder A apparently has smaller individual particle size, thus needing more heat to crystallize. Meanwhile, transformation from amorphous to anatase crystal structure for Powders B, C, and D occurred at

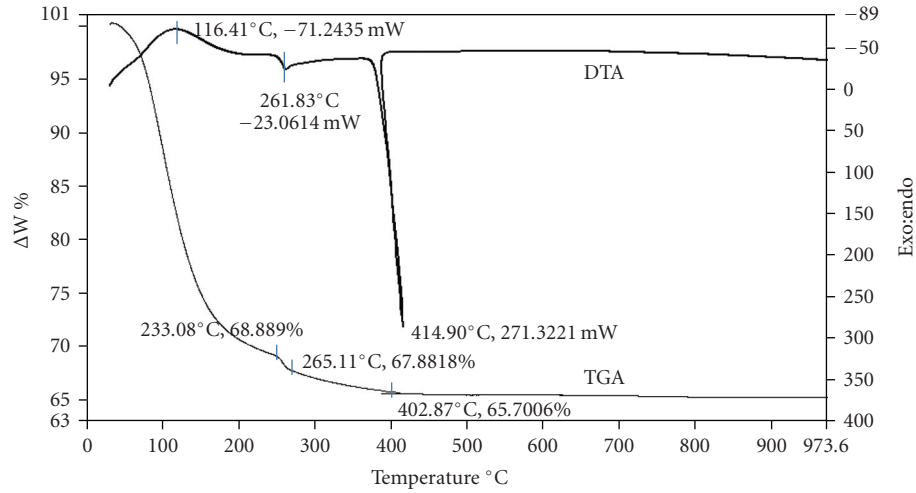

Figure 1: TG/DTA of TiO_2 Powder A.

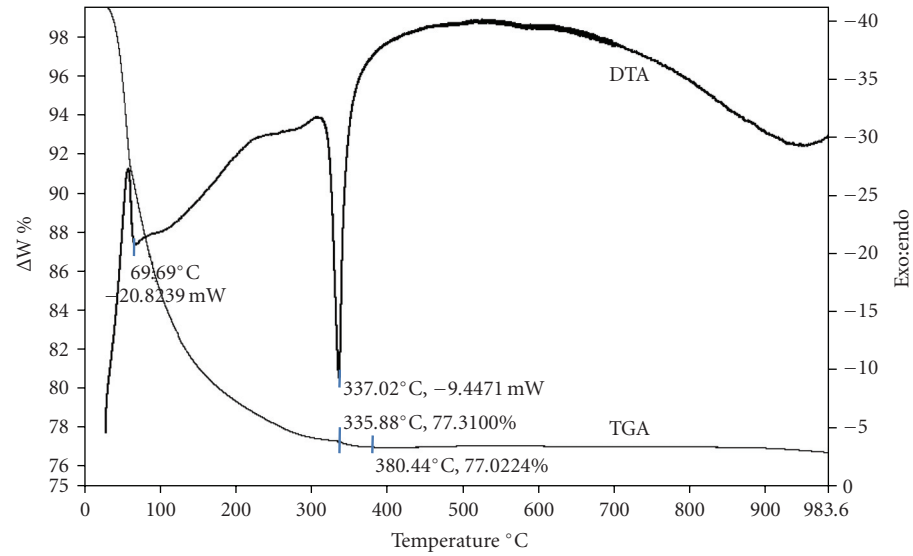

Figure 2: TG/DTA of TiO_2 Powder B.

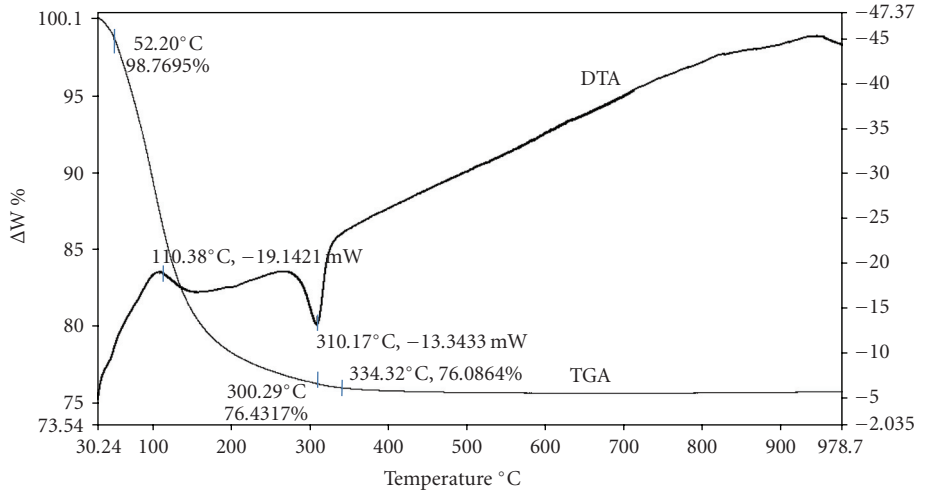

Figure 3: TG/DTA of TiO_2 Powder C.

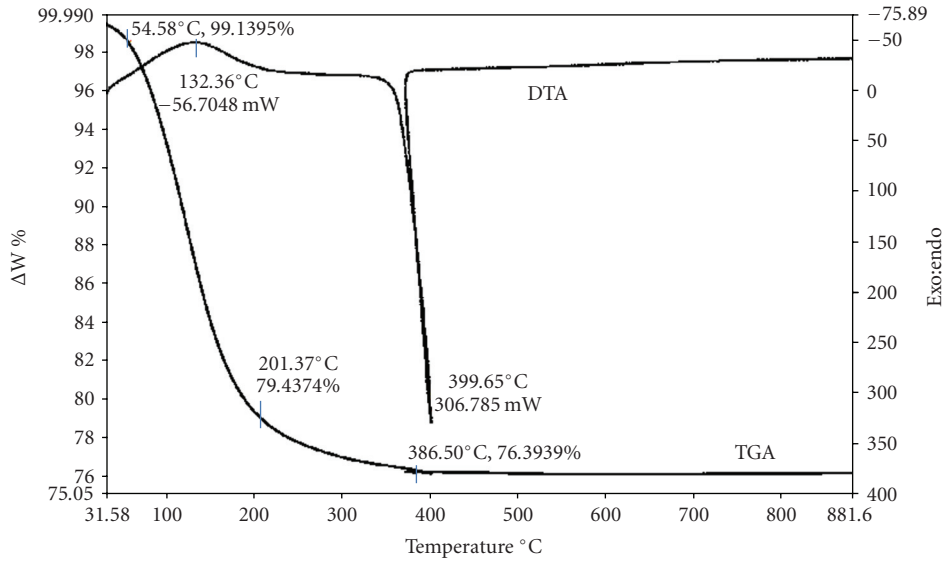

Figure 4: TG/DTA of TiO_2 Powder D.

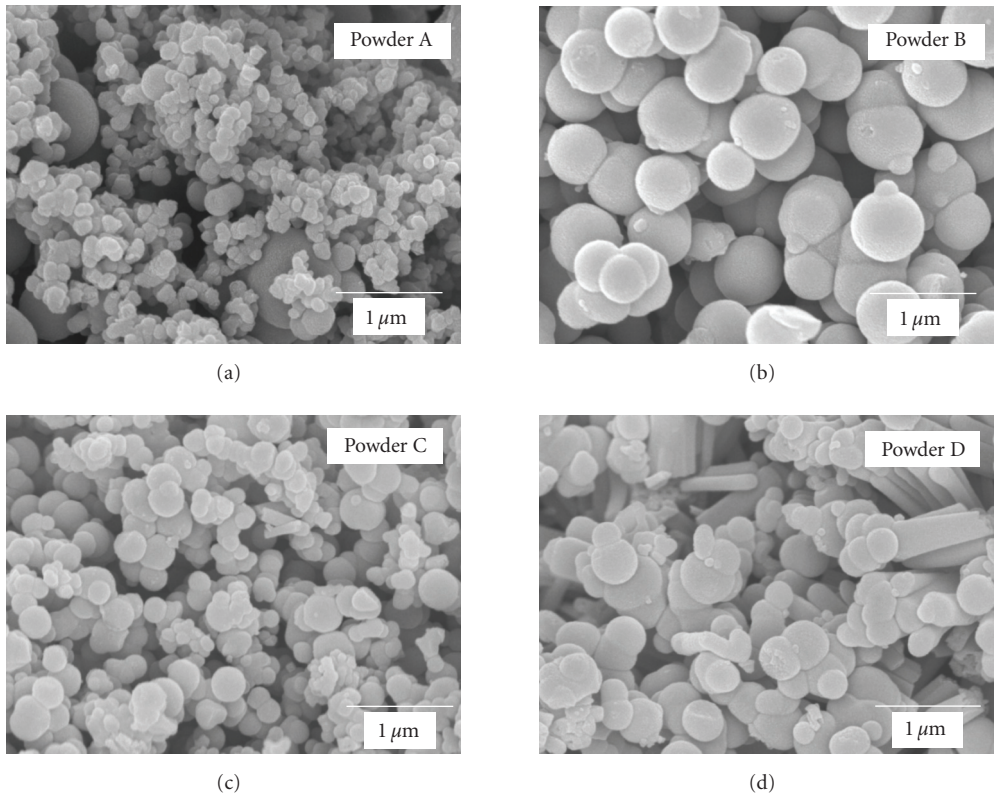

Figure 5: FESEM pictures of TiO_2 Powder A (water-to-TPT mol ratio of 1), Powder B (mol ratio of 2), Powder C (mol ratio of 3), and Powder D (mol ratio of 4).

lower temperatures (below 400°C) due to their large particles that needed less heat to crystallize. This finding can also be explained that when the mol ratio of water-to-TPT increased, crystallization temperature tends to be lower due to the formation of bigger particles. Figure 5 shows the surface morphology analysis by FESEM for TiO_2 Powders A, B, C, and D, respectively. The pictures showed that TiO_2 Powders A and B consist of spherical shaped particles, with particles B is larger than A. Less amount of water added slow down the polymerization process as the hydrolysis rate became less progressive. When the mol ratio of water-to-TPT increased to 3 and 4, hydrolysis and polymerization became more

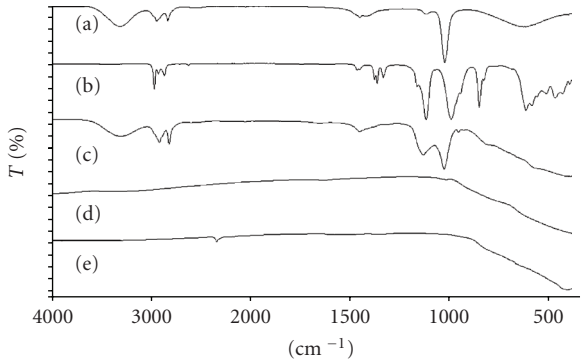

Figure 6: FTIR spectra of (a) methanol solution, (b) titanium (IV) isopropoxide, (c) TiO_2 powder after filtration process, (d) TiO_2 powder after drying at 200°C process, and (e) TiO_2 powder after calcination treatment at 400°C.

Table 1: Crystallization temperature of sol-gel TiO_2 powders as evaluated using the TG/DTA.

Sol-gel TiO_2	Mol ratio of water-to-TPT	Crystallization temperature (°C)
Powder A	1	414
Powder B	2	337
Powder C	3	310
Powder D	4	399

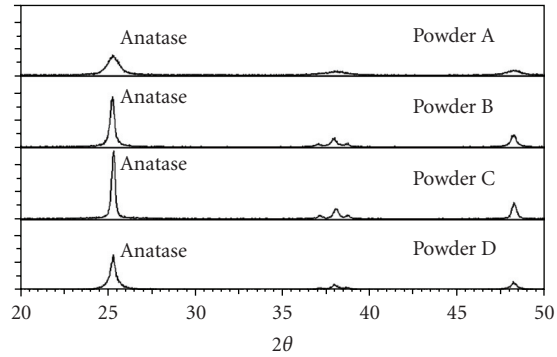

Figure 7: XRD patterns of sol-gel TiO_2 Powders A (water-to-TPT mol ratio of 1), B (mol ratio of 2), C (mol ratio of 3), and D (mol ratio of 4).

Table 2: Particle size of sol-gel TiO_2 powders calculated using Scherrer's equation.

Sol-gel TiO_2	Mol ratio of water-to-TPT	Degree in 2θ	Particle size (nm)
Powder A	1	25.3	10.8
Powder B	2	25.3	30.2
Powder C	3	25.4	37.1
Powder D	4	25.4	24.1

progressive which accelerated the TiO_2 phase formation rate. Rapid hydrolysis likely formed inhomogeneous nonspherical shape powder particles as shown by Powders C and D. Thus, the amount of water added during the synthesis process plays an important role in controlling the formation of TiO_2 particles.

It is important to note, a slower polymerization process and hydrolysis rate are required to produce smaller particle with more uniform size. It is preferable to have a uniform size of TiO_2 powder as it can control the degradation of organic molecule to happen at faster rate. With uniform particles size, it can increase the amount of pollutants molecules adsorbed on the catalyst's surface and increase its photocatalytic activity. Meanwhile, smaller powder particles will provide shorter distance to be traveled by the electrons from the valence band to the catalytic site. Hence, more holes will be left at the valence band by the electrons that move to the conduction band. The conduction band electrons are the reduction centers that will react with oxygen while the valence band holes become the oxidation centers that will react with water to produce more hydroxyl radicals.

Figure 6 shows the FTIR spectra for methanol (a), titanium tetraisopropoxide (b), TiO_2 gel powder (c), TiO_2 powder after drying at 200°C (d), and TiO_2 powder after calcination (e). In Figure 6(a), absorption peaks of methanol appear at 3314 cm^{-1} which is attributed to O-H stretching band and at 1113 cm^{-1} attributed to C-O stretching band. Figure 6(b) shows the FTIR spectra of titanium (IV) isopropoxide with absorbance peaks at 2942 cm^{-1} and 987 cm^{-1} belonged to aliphatic C-H stretching band and C-H alkene bending band, respectively. From Figure 6(c), it is clearly shown that the gel powder after filtration process resembled mixture of spectra of both chemicals. After drying at 200°C, all the bands disappeared and only Ti-O bond's weak stretching band at 394 cm^{-1} remained. This peak was stronger after the powder was calcined at 400°C showing a densified inorganic phase of TiO_2. It is important to note that the inorganic bond of Ti-O does not always exist at low wavenumber as reported here. Wang et al. [22] reported that their TiO_2 submicrospheres showed Ti-O stretching mode at higher wavenumber of 568 cm^{-1}.

From XRD analysis presented in Figure 7, all TiO_2 powders have the highest peak at 25° in 2θ indicating that the powders are purely anatase structure. No other peak other than anatase was identified from the analysis. It is noticed that as the mol ratio of water-to-TPT increased, the powder particles increased both in size and crystallinity. The XRD patterns prove that TiO_2 Powder A has the smallest particle size with low crystallinity while Powders B and C have the highest crystallinity but still maintaining its purity. As for Powder D, it has an intermediate crystallinity between Powders A and B. Theoretically, an increase in powder's crystallinity will lead to an increase in powder's particle size. From the XRD pattern, it is assumed that the particle size of Powder A is the smallest as it has the lowest crystallinity compared to Powder B, C, and D. The powder particle size is confirmed by Scherrer's equation calculation presented in Table 2.

Comparing TiO_2 Powders A, B, and D for further evaluation on the effect of hydrolysis rate on the powders'

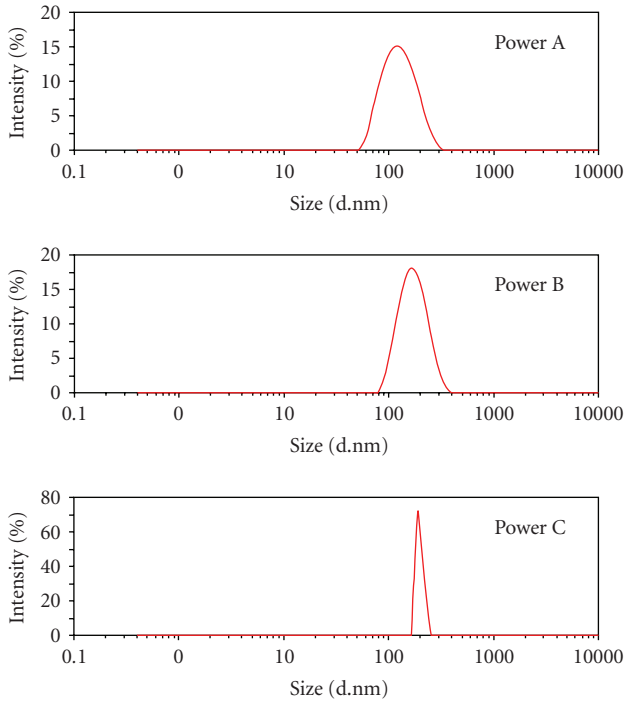

Figure 8: Particle size distribution of TiO_2 Powder A (water-to-TPT mol ratio of 1), Powder B (mol ratio of 2), and Powder D (mol ratio of 4).

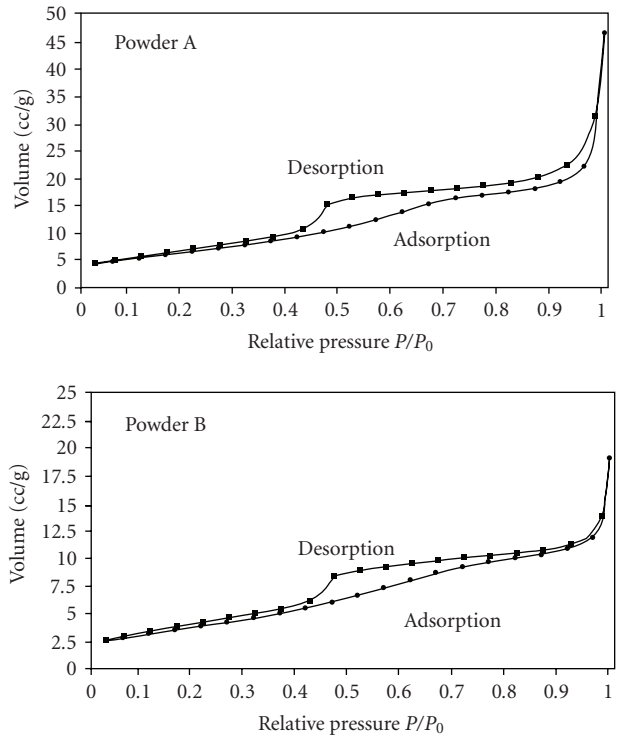

Figure 9: N_2 adsorption-desorption isothermal analysis of Powder A (water-to-TPT mol ratio of 1) and Powder B (water-to-TPT mol ratio of 2).

properties, it can be clearly seen that a small change in mol ratio of water-to-TPT affected the particles shape formed. Powder A that experienced slow hydrolysis rate has the smallest particles compared to Powders B and D due to less progressive hydrolysis. Meanwhile, TiO_2 Powder B has a higher crystallinity than Powders A and D while maintaining its purity as shown from XRD analysis. It should be noted that high crystallinity is also an important property for an efficient photodegradation. High crystallinity TiO_2 can produce more charge carriers to the catalytic site to degrade the organic molecules.

From the particle size analysis as shown in Figure 8, Powder A's mean particle size was 118 nm with particle size distribution ranging from 50 to 300 nm. The particle size of Powder B was ranging from 80 to 400 nm with the mean particle size of 167 nm. Powder D particles size range was from 150 nm to 500 nm with mean particle size of 199 nm. It is worthy to note that the particle size measured from this analysis was quite big in size due to the possibility that powder's agglomerates were measured instead of individual particles. In fact, most particles were dispersed into a primary size in aqueous suspension [23]. In addition, small particles tend to agglomerate due to its high surface energy to attract other particles to combine together and form large primary particles. Hence, it is presumed that particles are aggregated into agglomerates in this suspension.

BET surface area analysis shows that the sol-gel TiO_2 powders have Isotherm type II which was evaluated from the adsorption curves of Powders A and B shown in Figure 9. Type II isotherms are normal forms of isotherms obtained with a nonporous and macroporous adsorbent. The hysteresis loop formed by the adsorption-desorption curve indicates that both powders had type E hysteresis loop that can be attributed to "ink-bottle" pores. From BET surface area analysis, Powders A and Powder B have surface area of 24.8 m^2/g and 14.6 m^2/g, respectively. This BET result is consistent with the results from XRD, FESEM, and particle size analysis that Powder A has much smaller mean particles size than Powder B.

3.2. Photocatalytic Measurement. Photocatalytic degradation of phenol using TiO_2 Powders A, B, and D has been conducted under UV irradiation of 2.6 mW/cm^2 intensity. In this case, 5 g of TiO_2 powders were mixed with 250 mL of phenol solution with initial concentration of 50 mg/L. The suspension was stirred to obtain the maximum adsorption of organic pollutant molecules on the photocatalyst surface and then exposed to UV irradiation for 5 hours. The sampling was taken every one hour and filtered to remove the excess of TiO_2 powders to get a clear solution prior to UV-Vis spectrometer measurement.

The plots showing phenol degradation by these three TiO_2 powders are presented in Figure 10. It was found that TiO_2 Powder B showed the fastest degradation compared to Powders A and D. Powder B managed to degrade ca. 50% of the phenol initial concentration within the first 60 minutes. It can be observed that rate of phenol degradation by Powder A was very slow and almost constant for the whole 5 hours. About 77% of the initial concentration has been completely degraded by TiO_2 Powder B after 5 hours compared to only 26% by Powder A and 57% by Powder D.

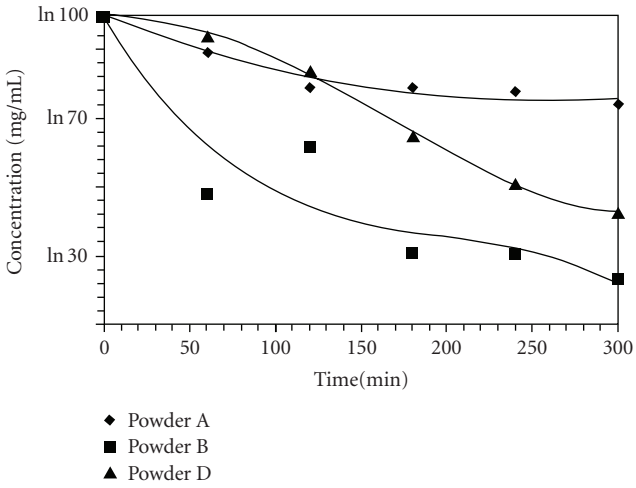

Figure 10: Plots showing concentration versus irradiation time in the degradation of phenol using Powders A, B, and D.

Some researchers claimed that smaller particle size of powder can lead to faster degradation of organic compound than bigger particles. However, Kanipus et al. [24] reported that degradation rate did not depend on specific surface area of TiO_2. The influence of the TiO_2 crystalline structure is stronger for the transformations of inorganic anions whereby the rate constants can differ in 30 times. In this research TiO_2 Powder B showed the fastest degradation of phenol in solution due to its high crystallinity than Powder A and D. This is due to the Powder B's optimum crystallinity and particle size that could lead to an efficient removal of phenol. This optimum crystallinity was responsible to form more charge carriers at the photocatalyst's surface to enhance the photocatalytic efficiency. Thus, higher crystallinity of Powder B could compensate its large particles to perform faster photocatalytic process. The low efficiency of Powder A in photodegradation process of phenol molecules can be explained by its small particle size. The solution was clouded by small particles of Powder A and did not permit the maximum UV to penetrate into the solution. If the powder particles are too small, it can create "screening effect" in the solution that can limit the penetration of UV light into the solution and slow down the degradation rate [25]. This argument is also supported by Hosseini et al. [26] that the presence of $^{\bullet}O_2^-$ and the $^{\bullet}OH$ radicals depend both on photocatalyst surface and solution composition. This research proves that TiO_2 powder with high crystallinity also shows high potential to degrade organic compound. Kinetic analysis for photocatalytic degradation of phenol under optimal conditions parameters still needs to be carried out for further investigation.

4. Conclusion

Sol-gel TiO_2 powders with the water-to-TPT mol ratios of 1 (Powder A), 2 (Powder B), 3 (Powder C), and 4 (Powder D) were synthesized and their physicochemical properties were evaluated. All powders are 100% in anatase structure. Powder A with the smallest individual particles needed more heat energy to become crystalline due to its smaller particle size than Powders B, C, and D. The powder started to form homogeneous spherical shape to inhomogeneous shape as the water-to-TPT mol ratio increased. It was proven that the amount of water added during synthesis process could affect the hydrolysis-polymerization rate and consequently the particle size and shape. Powder's crystallinity became higher when the mol ratio of water-to-TPT was increased due to the acceleration of hydrolysis rate during the synthesis process. From the photocatalytic degradation of phenol, Powder B showed the fastest phenol degradation and higher efficiency than Powders A and D due to its high crystallinity that was capable of producing more charge carriers at the catalyst's surface to degrade the adsorbed phenol molecules.

Acknowledgment

The authors acknowledge the Ministry of Higher Education of Malaysia (MOHE) for their financial support (Research no. FRGS 0106-22).

References

[1] O. Zahraa, L. Sauvanaud, G. Hamard, and M. Bouchy, "Kinetics of atrazine degradation by photocatalytic process in aqueous solution," *International Journal of Photoenergy*, vol. 5, no. 2, pp. 87–93, 2003.

[2] S. K. Kansal, M. Singh, and D. Sud, "Studies on photodegradation of two commercial dyes in aqueous phase using different photocatalysts," *Journal of Hazardous Materials*, vol. 141, no. 3, pp. 581–590, 2007.

[3] M. Krichevskaya, A. Kachina, T. Malygina, S. Preis, and J. Kallas, "Photocatalytic oxidation of fuel oxygenated additives in aqueous solutions," *International Journal of Photoenergy*, vol. 5, no. 2, pp. 81–86, 2003.

[4] V. Augugliaro, C. Baiocchi, A. B. Prevot, et al., "Azo-dyes photocatalytic degradation in aqueous suspension of TiO_2 under solar irradiation," *Chemosphere*, vol. 49, no. 10, pp. 1223–1230, 2002.

[5] http://www.epa.gov.

[6] K. M. Parida, N. Sahu, N. R. Biswal, B. Naik, and A. C. Pradhan, "Preparation, characterization, and photocatalytic activity of sulfate-modified titania for degradation of methyl orange under visible light," *Journal of Colloid and Interface Science*, vol. 318, no. 2, pp. 231–237, 2008.

[7] T. Kudo, Y. Nakamura, A. Ruike, and A. Hasegawa, "Design and development of highly efficient rectangular column structured titanium oxide photocatalysts anchored onto silica sheets," *Topics in Catalysis*, vol. 35, no. 3-4, pp. 225–229, 2005.

[8] M. N. Rashed and A. A. El-Amin, "Photocatalytic degradation of methyl orange in aqueous TiO_2 under different solar irradiation sources," *International Journal of Physical Sciences*, vol. 2, no. 3, pp. 73–81, 2007.

[9] O. Prieto, J. Fermoso, and R. Irusta, "Photocatalytic degradation of toluene in air using a fluidized bed photoreactor," *International Journal of Photoenergy*, vol. 2007, Article ID 32859, 8 pages, 2007.

[10] W. Su, J. Chen, L. Wu, X. Wang, X. Wang, and X. Fu, "Visible light photocatalysis on praseodymium(III)-nitrate-modified TiO_2 prepared by an ultrasound method," *Applied Catalysis B*, vol. 77, no. 3-4, pp. 264–271, 2008.

[11] F. Chen, J. Zhao, and H. Hidaka, "Highly selective deethylation of rhodamine B: adsorption and photooxidation pathways of the dye on the TiO_2/SiO_2 composite photocatalyst," *International Journal of Photoenergy*, vol. 5, no. 4, pp. 209–217, 2003.

[12] H. Yang, K. Zhang, R. Shi, X. Li, X. Dong, and Y. Yu, "Sol-gel synthesis of TiO_2 nanoparticles and photocatalytic degradation of methyl orange in aqueous TiO_2 suspensions," *Journal of Alloys and Compounds*, vol. 413, no. 1-2, pp. 302–306, 2006.

[13] H. Yin, Y. Wada, T. Kitamura, et al., "Hydrothermal synthesis of nanosized anatase and ruffle TiO_2 using amorphous phase TiO_2," *Journal of Materials Chemistry*, vol. 11, no. 6, pp. 1694–1703, 2001.

[14] M. Sakanoue, Y. Kinoshita, Y. Otsuka, and H. Imai, "Photocatalytic activities of rutile and anatase nanoparticles selectively prepared from an aqueous solution," *Journal of the Ceramic Society of Japan*, vol. 115, no. 1348, pp. 821–825, 2007.

[15] M. H. Habibi, A. Hassanzadeh, and S. Mahdavi, "The effect of operational parameters on the photocatalytic degradation of three textile azo dyes in aqueous TiO_2 suspensions," *Journal of Photochemistry and Photobiology A*, vol. 172, no. 1, pp. 89–96, 2005.

[16] H. Vosooghian and M. H. Habibi, "Photooxidation of some organic sulfides under UV light irradiation using titanium dioxide photocatalyst," *International Journal of Photoenergy*, vol. 2007, Article ID 89759, 7 pages, 2007.

[17] M. H. Habibi, N. Talebian, and J.-H. Choi, "The effect of annealing on photocatalytic properties of nanostructured titanium dioxide thin films," *Dyes and Pigments*, vol. 73, no. 1, pp. 103–110, 2007.

[18] M. H. Habibi and N. Talebian, "Photocatalytic degradation of an azo dye X6G in water: a comparative study using nanostructured indium tin oxide and titanium oxide thin films," *Dyes and Pigments*, vol. 73, no. 2, pp. 186–194, 2007.

[19] C.-W. Lee and J.-S. Lee, "Formation of TiO_2 hollow nanoparticles via gas phase synthesis using titanium oxide acetylacetonate as a precursor," *Journal of the Ceramic Society of Japan*, vol. 114, no. 1335, pp. 923–928, 2006.

[20] M. Inada, K. Kamada, N. Enomoto, and J. Hojo, "Microwave effect for synthesis of TiO_2 particles by self-hydrolysis of $TiOCl_2$," *Journal of the Ceramic Society of Japan*, vol. 114, no. 1334, pp. 814–818, 2006.

[21] M. Zhang, J. Wang, and H. Fu, "Preparation and photocatalytic activity of nanocrystalline TiO_2 with uniform shape and size," *Journal of Materials Processing Technology*, vol. 199, no. 1, pp. 274–278, 2008.

[22] H. Wang, B. Li, Z. Yan, Z. Lu, R. Cheng, and D. Qian, "Fast synthesis of monodisperse TiO_2 submicrospheres via a modified sol-gel approach," *Rare Metals*, vol. 27, no. 1, pp. 1–4, 2008.

[23] J. Imasu and Y. Sakka, "Large-scale patterning of TiO_2 nano powders using micro molds," *Journal of the Ceramic Society of Japan*, vol. 115, no. 1347, pp. 697–700, 2007.

[24] E. I. Kapinus, T. A. Khalyavka, V. V. Shimanovskaya, T. I. Viktorova, and V. V. Strelko, "Photocatalytic activity of spectro-pure titanium dioxide: effects of crystalline structure, specific surface area and sorption properties," *International Journal of Photoenergy*, vol. 5, no. 3, pp. 159–166, 2003.

[25] S. K. Kansal, M. Singh, and D. Sud, "Comparative evaluation of UV/solar light induced photodegradation of phenol in aqueous solutions," *Indian Chemical Engineer*, vol. 49, no. 1, pp. 11–20, 2007.

[26] S. N. Hosseini, S. M. Borghei, M. Vossoughi, and N. Taghavinia, "Immobilization of TiO_2 on perlite granules for photocatalytic degradation of phenol," *Applied Catalysis B*, vol. 74, no. 1-2, pp. 53–62, 2007.